Effect of fracture characteristics on DNAPL-water flow in rock fractures

W. M. S. B. Weerakone
Golder Associates Ltd., Calgary, Alberta, Canada
R. C. K. Wong
Department of Civil Engineering, University of Calgary, Alberta, Canada

ABSTRACT
This study investigates the influence of fracture properties on Dense Non-Aqueous Phase Liquids (DNAPL)-water flow in rock fractures. The aperture distributions of fractures in sandstone and shale specimens of Alberta Paskapoo Formation were obtained from X-ray Computed Tomography (CT) technique. Then, geostatistical parameters of each aperture distribution were estimated, and isotropic or anisotropic nature of the aperture distributions were identified. Equiprobable aperture distributions were generated from stochastic simulation to observe the effect of anisotropy of aperture distribution on DNAPL migration parameters. First, pore-scale single-phase flow was simulated in generated fractures using classical Local Cubic Low (LCL) approach. Then, DNAPL-water two-phase flow process was simulated in each generated fracture by utilizing the invasion percolation approach. The effects of anisotropy of aperture distributions on the main flow parameters, the fracture permeability and capillary pressure–saturation relationship, were determined from the results of the simulated flow processes.

RÉSUMÉ
Cette étude a examiné l'influence des propriétés des fractures sur les phases liquides denses non-aqueux (DNAPL) - particulièrement l'écoulement le long de fractures de roche. La distribution des ouverture des fractures dans des spécimens de grès et de schiste de la formation Paskapoo en Alberta ont été examinés utilisant la technique de la tomographie rayon X (CT). Puis, des paramètres geostatistiques de chacune des ouvertures ont été estimés pour en identifier la nature isotrope ou anisotrope. Des distributions d'ouverture d'équiprobable ont été produites pour observer l'effet de l'anisotropie sur les paramètres de migration du DNAPL. Premièrement, l'écoulement monophasé dans les fractures a été simulé en utilisant l'approche (LCL) cubique locale classique. Ensuite, le procédé biphasé d'écoulement du DNAPL a été simulé dans chaque fracture produite en utilisant l'approche de percolation d'invasion. Les effets de l'anisotropie des distributions d'ouverture sur les paramètres principaux d'écoulement, la perméabilité de la fracture et rapport de pression-saturation capillaire, ont été déterminés à partir des résultats de simulation.

1 INTRODUCTION

Rock fracture is a crucial geological feature in subsurface contaminant migration process. The effects of fracture characteristics on migration process of Dense Non-Aqueous Phase Liquids (DNAPL), a critical ground water contaminant in many industrialized cities, are the main focus of this study. The investigation is restricted for single rock fractures, which act as the fundamental elements in understanding the flow behavior in fracture networks.

1.1 Fracture Aperture Distribution

Determination of aperture distribution is essential to estimate the fracture characteristics and flow behavior of a single fracture. Some early researches proposed to estimate the aperture distribution by obtaining a cast of the void space. In several other studies fracture replicas were first constructed from a transparent material and the aperture distribution was determined by means of light transmission. The use of a profilometer or a nuclear magnetic resonance imaging (NMRI) technique is another method of measuring the fracture apertures. X-ray computer tomography (CT) is an attractive technique for determination of morphology of rock fractures (Johns et al., 1993; Keller, 1997; Bertels et al., 2001; Muralidharan et al., 2004; Walters, 1995) due to its convenience of use and non-destructive nature.

Goestatistics have been used in studies of single fractures for characterization of fracture surfaces (Marache et al., 2002) or for generation of aperture distributions (Moreno et al., 1988; Tsang and Tsang, 1989; Pruess and Tsang, 1990). The spatial continuity is an important property of a fracture aperture distribution and it can be quantitatively estimated by geostatistical parameters.

1.2 DNAPL-Water Flow In Rock Fracture

The DNAPLs migrate deep into the subsurface due to their high densities and accumulate on the bedrock. If the bedrock is fractured, DNAPLs can enter into the fractures. However, for entry, the DNAPL pressure has to be higher than the capillary forces between water and DNAPL at the fracture entrance (Kueper and McWhorter, 1991). Once entered, the migration of DNAPL in variable aperture fractures is controlled by the capillary forces (Reitsma and Kueper, 1994). The capillary pressure, the pressure difference between water and DNAPL, governs the DNAPL saturation in the fracture. Hence, the relationship between capillary pressure and saturation is a vital

parameter in the DNAPL migration process (Kueper and McWhorter, 1991).

2   FRACTURE APERTURE DISTRIBUTIONS

The rock samples for this study were obtained from the Paskapoo formation of south-western Alberta; a sedimentary rock formation composed dominantly of shale and sandstone. A 142 mm diameter, 276 mm long, sandstone specimen and 75 mm diameter, 120 mm long, sandstone and shale specimens were used in fracture aperture measurements. The reasons for selecting three different specimens were to observe the effect of specimen size and rock type on aperture distribution.

Extraction of naturally fractured samples is rather expensive and time consuming. Therefore, intact sandstone and shale samples were obtained and fractures were induced in the laboratory in the specimens cored to necessary size and shape.

The fracturing method used in this study is similar to the Brazilian tensile fracturing technique. An uniaxial compression device was used for the fracturing. The specimens were set on the loading machine with their axis horizontal. Two steel rods of ½ inch (12.7 mm) diameter were placed on the top and bottom of the specimen and load was applied on the steel rods. Two steel plates were positioned vertically at two sides of the specimen and bolted together at the ends. These side plates helped to create a single fracture, between the top loading point and the bottom loading point without any shear fractures. Further, they prevented the separation of the specimen into two halves at the end of fracturing. The load was increased at a very slow rate. The loading was stopped just after a vertical fracture propagated through the specimen, and then the specimen was removed from the machine without disturbing the fracture.

After the fracture generation, an epoxy shell was cast around the 142 mm diameter sandstone specimen to keep two pieces of the specimen together. The two 75 mm diameter fractured specimens, were kept intact using rubber membranes.

The X-ray CT scanning technique was used to measure the aperture distribution of the rock fractures. First, the calibration curves were developed from known aperture fractures. The specimens were scanned perpendicular to their axis to obtain series of CT images to cover the full fracture length. The developed calibration curves were utilized to transform the information in the CT images into fracture aperture values (Weerakone and Wong, 2007). Figure 1 shows the developed two dimensional aperture distribution map for the 142 mm diameter sandstone specimen. Three dimensional views of fractures were developed to compare the undulations of the fractures and Figures 2 and 3 illustrate those of 75 mm sandstone and shale specimens.

Colour key for aperture values (mm)

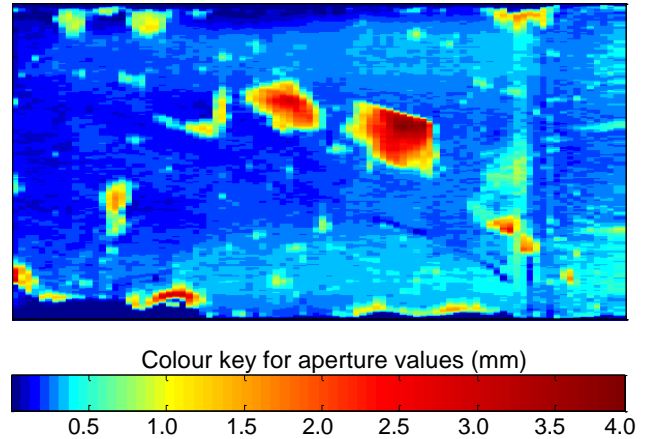0.5   1.0   1.5   2.0   2.5   3.0   3.5   4.0

Figure 1. Aperture distribution of the fracture in 142 mm diameter sandstone specimen
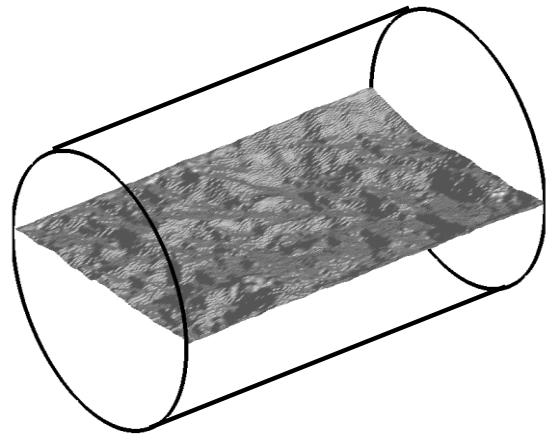

Figure 2. Three dimensional view of the fracture in 75 mm diameter sandstone specimen
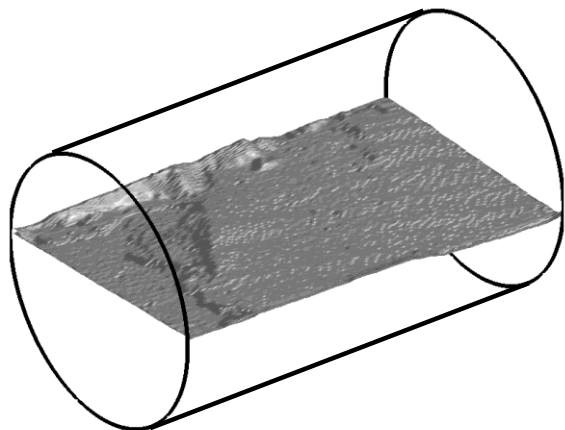

Figure 3. Three dimensional view of the fracture in 75 mm diameter shale specimen

No significant differences were observed in the fractures of the two sandstone specimens. That illustrates the effect of specimen size on aperture distribution is small. However, there were significant differences between fractures in sandstone and shale specimens. The two dimensional aperture distribution of the fracture in the shale specimen illustrated less variation and the three dimensional view of the same fracture demonstrated less undulation compared to that of the sandstone specimen. The layered structure and the fine grains in shale specimen may be the cause for the above mentioned observations.

3   GEOSTATISTICAL PROPERTIES

The variation of spatial continuity in different directions of an aperture distribution was analyzed using directional variograms. The variogram of a data set in a particular direction can be obtained from;

$$\gamma(h) = \frac{1}{2N(h)} \sum_{(i,j)|h_{ij}=h} (v_i - v_j)^2 \qquad [1]$$

where v_1, v_2, ...v_i, ...v_j,...v_n are the data values and $N(h)$ is the number of data pairs used in the summation. The locations of data points in each pair are separated by h distance and they are in the direction of h (Isaaks and Srivastava, 1989).

The variograms were determined for eight different directions for each aperture distribution. Figure 4 demonstrates two such variograms in directions parallel and perpendicular to the specimen axis for the aperture distribution of the fracture in the 75 mm diameter sandstone specimen.
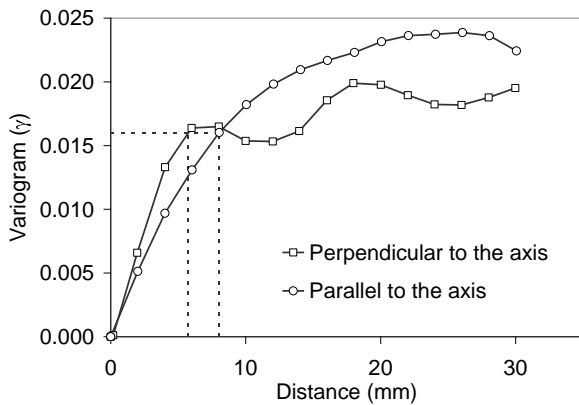

Figure 4. Variograms parallel and perpendicular to the specimen axis for the aperture distribution of the fracture in the 75 mm diameter sandstone specimen

The distance required to achieve a particular variogram value in each directional variogram was determined and the estimated distances were plotted with their corresponding directions. An ellipse was fit to the diagram to identify the anisotropy of the measured aperture distributions. This type of diagram is generally referred to as rose diagram. Figure 5 illustrates the rose diagram for the aperture distribution of the fracture in 75 mm diameter sandstone specimen. Analogous diagrams were developed for all three fractures and similar behaviors were observed.

The directions of the major and minor axes of the fitted ellipse were considered as the maximum and minimum continuity directions, respectively. The direction of the maximum continuity is referred to as the axis of anisotropy (Isaaks and Srivastava, 1989).

According to the results, the three measured aperture distributions consistently illustrated anisotropy with highest continuity in the direction parallel to the specimen axis. Therefore, it was decided to investigate the effect of the anisotropy of the aperture distribution on DNAPL-water flow process.
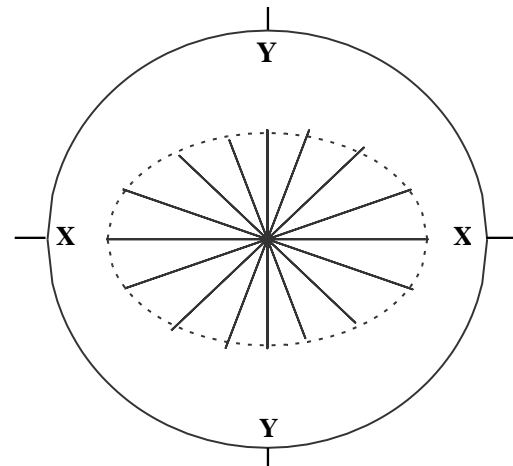

Figure 5. The rose diagram for the aperture distribution of the fracture in 75 mm diameter sandstone specimen (XX direction is parallel to the specimen axis and YY direction is perpendicular to the specimen axis)

The anisotropy in an aperture distribution is caused by different reasons, including the internal grain structure of the rock specimen and the fracturing mechanism used in the experiments. In this study, the fractures were generated parallel to the natural bedding planes of the specimens. Still fractures ran through several layers of the rock specimen. When the fractures passed through different layers, they were frequently observed in the direction perpendicular to specimen axis, compared to the direction parallel to the specimen axis. That resulted in reduced continuity of aperture distribution in the direction perpendicular to the axis. During the fracturing process, the load was applied in the direction perpendicular to the specimen axis while restricting expansions at the two sides of the specimens. This loading procedure must

have led to the higher variation in aperture distribution in the direction perpendicular to specimen axis compared to the direction parallel to the specimen axis.

4   STOCHASTIC SIMULATIONS

The stochastic simulation techniques in geostatistics are capable of generating alternative equiprobable aperture distributions for measured fractures. In this study such simulated aperture distributions were utilized to observe the effect of anisotropy of aperture distribution on DNAPL migration in rock fractures. The sequential Gaussian simulation method with simple kriging was used in all simulations (Deutsch and Journel, 1998).

The properties of the measured aperture distribution of the fracture in the 142 mm diameter sandstone specimen were used in the simulations to obtain analogous aperture distributions. First five simulations used the same variograms as in the measured aperture distribution which possessed the longest spatial continuity parallel to specimen axis and the shortest spatial continuity perpendicular to the specimen axis. The variograms were interchanged in the next five simulations. Figure 7 shows one aperture distribution from the first five realizations and Figure 8 shows one aperture distribution from the next five realizations.

Simulated aperture distributions should have statistical properties similar to these of the measured aperture distributions. Therefore, the statistical properties, the variograms and the quantile-quantile plots were compared to judge the compatibility of the simulated aperture distribution to the measured aperture distribution. The generated aperture distributions demonstrate high compatibilities within reasonable statistical fluctuations.

Color key of aperture values (mm)

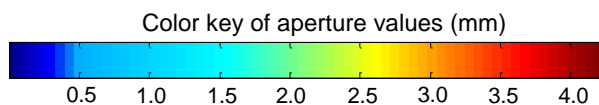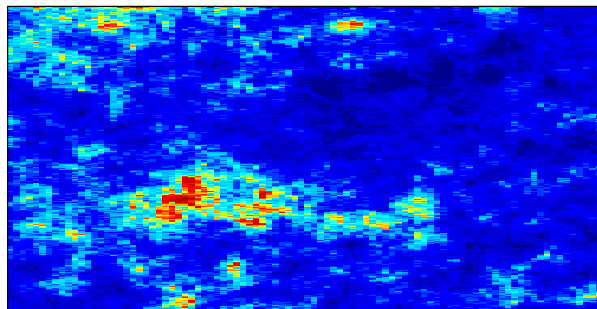0.5   1.0   1.5   2.0   2.5   3.0   3.5   4.0

Figure 6. One realization from the first five fracture simulations in which the longest spatial continuity is parallel to the specimen axis

Color key of aperture values (mm)

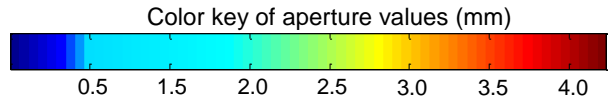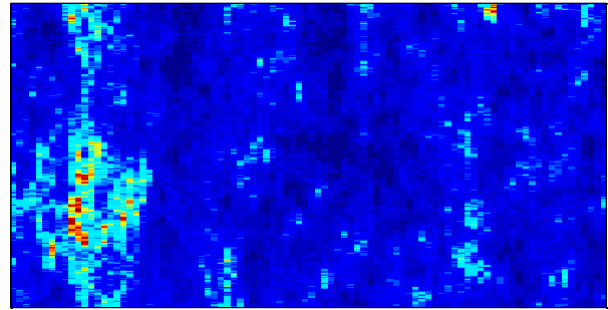0.5   1.5   2.0   2.5   3.0   3.5   4.0

Figure 7. One realization from the second five fracture simulations in which the longest spatial continuity is perpendicular to specimen axis

5   SINGLE-PHASE FLOW

Pore-scale simulation of single-phase flow was conducted in geostatistically generated fractures to observe the effects of properties of fracture aperture distribution on single-phase flow behaviour. The classical local cubic law (LCL) approach was used to simulate the single-phase flow in six different fractures. Three fractures were selected from first five fracture simulations, which possess a high spatial continuity in aperture values in the flow direction, and another three fractures were selected from second five fracture simulations, which possess a high spatial continuity in aperture values perpendicular to the flow direction.

The flow between two smooth parallel plates can be calculated from the well known "cubic law". The cubic law for a horizontal parallel plate fracture is given by Equation [2].

$$Q = -W \frac{h^3}{12\mu} \frac{dp}{dx} \qquad\qquad [2]$$

The volumetric flow rate, Q, is proportional to the cube of the fracture aperture, h. The variables W, μ and dp/dx represent the width of the fracture, viscosity of the fluid and pressure gradient of the fluid along the fracture respectively. In classical local cubic law approach, the fracture elements of an aperture distribution are assumed as parallel plate fractures and the fracture is considered as a collection of such parallel plate elements in a horizontal plane. Then, cubic law can be applied to these parallel plate fracture elements.

First the governing equations were derived for the flow problem and then they were solved using the "control volume" approach of finite difference numerical method.

The two long edges of each fracture were considered as no flow boundaries. The fluid was injected from the left side edge and discharged from the right side edge. In all simulations the flow in rock matrix was assumed to be negligible compared to the flow in the fracture.
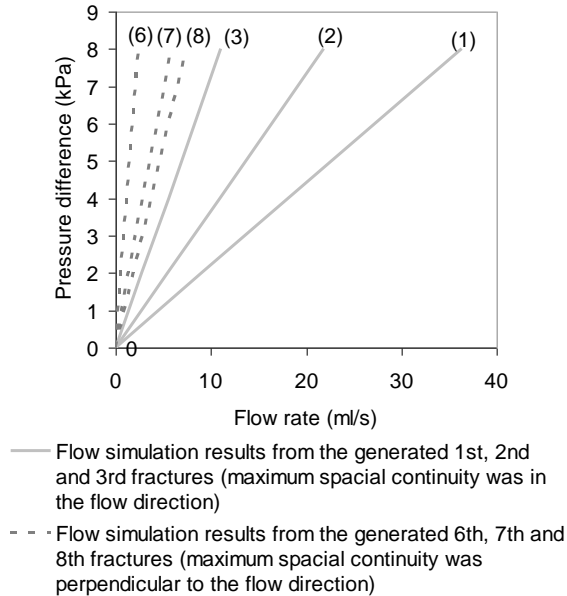

Figure 8. The results of the single-phase flow simulations in the fractures generated from geostatistical methods

The simulation results are illustrated in Figure 8. The results illustrates that when the spatial continuity of aperture distribution is high in the flow direction, the relationship between the flow rate and the pressure difference possess a low gradient (i.e., a high permeability) and when the spatial continuity of the aperture distribution is perpendicular to the flow direction, the above relationship has a high gradient (i.e., a low permeability). The results of this analysis demonstrated that the amount of the spatial continuity in the aperture values affect the fracture permeability at single-phase flow situations.

6   CAPILLARY PRESSURE CURVES

The generated aperture distributions and measured aperture distribution were used to simulate the capillary forces controlled DNAPL migration process. The capillary pressure-saturation relationships for each fracture were generated from the results of the flow simulations.

The trichloroethylene (TCE) was considered as the DNAPL for the simulation purpose and the interfacial tension between TCE and water was considered as 34.5 mN/m. A source of TCE was connected to one end of the water saturated fracture and the other end of the fracture was connected to a source of water through a capillary barrier. It was assumed that there was no flow through the two boundaries parallel to the axis of the specimen.

Each element of the fracture was assumed as a smooth parallel surface fracture.

The invasion percolation approach was used in flow simulations. The capillary pressure between two fluids was gradually increased, starting from zero, to allow DNAPL to invade the fracture. The DNAPL invades a fracture element only if the applied capillary pressure is equal or grater than the entry pressure of the fracture element as defined by the following Young-Laplace equation (Bertels et al., 2001).

$$P_c = \frac{2 \, \sigma \cos\theta}{b} \qquad\qquad [3]$$

The capillary pressure required to invade a fracture element of aperture b is defined by Pc. The σ and θ denote the interfacial tension and the contact angle between the two fluids, respectively. In addition to the above criterion, for the DNAPL invasion, there should be a continuous DNAPL path to the fracture element from the DNAPL source. During the DNAPL invasion, if water is trapped in some fracture elements surrounded by DNAPL, it is assumed that water can escape through the rock matrix. Figures 9 and 10 show the determined capillary pressure curves for the measured aperture distribution and generated realizations, respectively.

The breakthrough capillary pressure, the pressure at which the non-wetting phase maintains a continuous path throughout the fracture, is an important parameter in a capillary pressure curve. Table 1 illustrates the breakthrough capillary pressures for each generated realization.

When the DNAPL flows in the direction of high continuity of the aperture distribution, the breakthrough occurs at a lower capillary pressure compared to a flow in the less continuity direction. The results confirm that the flow direction affects the properties of the capillary pressure curve of an anisotropic fracture.
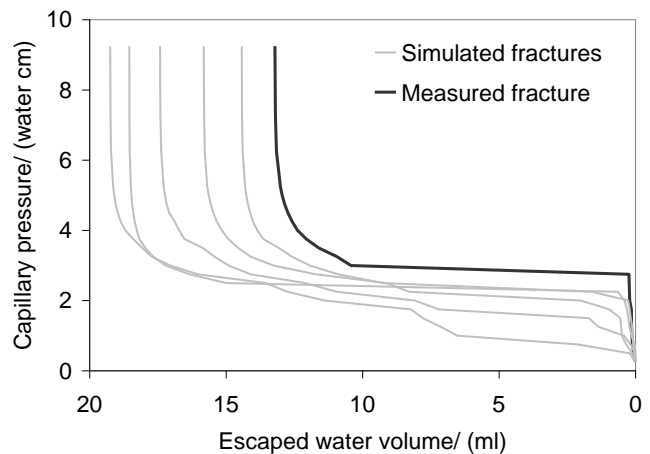

Figure 9. The capillary pressure curves for the measured aperture distribution and the first five simulated aperture distributions
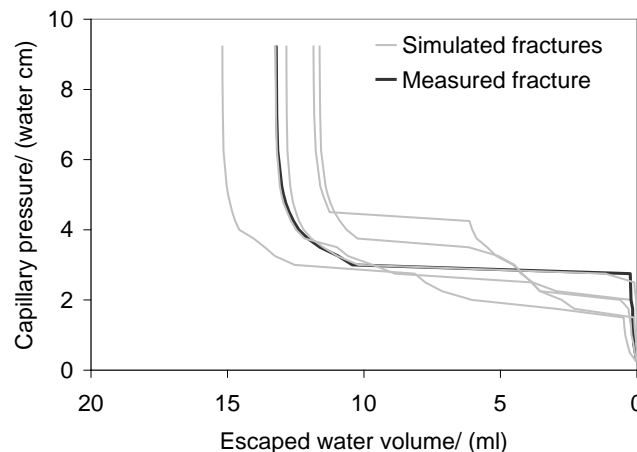
Figure 10. The capillary pressure curves for the measured aperture distribution and the second five simulated aperture distributions

Table 1: The breakthrough capillary pressure values of the simulated fracture apertures

Fracture	Direction of maximum continuity (with respect to specimen axis)	Breakthrough capillary pressure (water centimeters)
Simulation 1	Parallel	27.5
Simulation 2	Parallel	25
Simulation 3	Parallel	25
Simulation 4	Parallel	27.5
Simulation 5	Parallel	22.5
Simulation 6	Perpendicular	45
Simulation 7	Perpendicular	32.5
Simulation 8	Perpendicular	37.5
Simulation 9	Perpendicular	30
Simulation 10	Perpendicular	30

7   CONCLUSIONS

This study presents measured aperture distributions of different size and different type rock samples. The measured data reveal that the properties of rock fractures highly depend on the rock type, and the aperture distributions of the rock fractures have an anisotropic nature. The single-phase flow simulations in geostatistically generated fractures depict that high spatial continuity of aperture distribution in flow direction leads to a high fracture permeability. The results from the simulations of capillary forces dominant flow processes demonstrate that the breakthrough capillary pressure depends on the flow direction in an anisotropic fracture. It illustrates that the anisotropy of an aperture distribution affects the properties of the capillary pressure curve.

REFERENCES

Bertels, S. P., DiCarlo, D. A., and Blunt, M. J. 2001. Measurement of aperture distribution, capillary pressure, relative permeability, and in-situ saturation in a rock fracture using computed tomography scanning, *Water Resources Research*, 37(3): 649-662.

Deutsch, C. V., and Journal, A. G. 1998. *GSLIB Geostatistical software library and user's guide*, Oxford university press, New York, USA.

Isaaks, E. H., and Srivastava, R. M. 1989. *An introduction to applied geostatistics*, Oxford university press, New York, USA.

Johns, R. A., Steude, J. S., Castanier, L. M., and Roberts, P. V. 1993. Nondestructive measurements of fracture aperture in crystalline rock cores using X -ray computed tomography, *Journal of geophysical research*, 98: 1889-1900.

Keller, A. A. 1997. High resolution CAT imaging of fractures in consolidated materials, *International Journal of Rock Mechanics and Mining Science*, 34(3/4): 358-371.

Kueper, B. H., and McWhorter, D. B. 1992. The behavior of Dense, Nonaqueous phase liquids in fractured clay and rock, *Groung water*, (29)5: 716-728.

Marache, A., Riss, J., Gentier, S., and Chiles, J. P. 2002. Characterization and reconstruction of a rock fracture surface by geostatistics, *International journal for numerical and analytical methods in geomechanics*, (26): 873–896.

Moreno, L., Tsang, Y. W., Tsang, C. F., Hale, F. V., and Neretnieks, I. 1988. Flow and tracer transport in a single fracture-a stochastic model and its relation to some field observations, *Water Resources Research*, 24(12): 2033-2048.

Muralidharan, V., hakravarthy, D., Putra, E., and Schechter, D. S. 2004. Investigating fracture aperture distribution under various stress conditions using X-ray CT scanner, SPE 2004-230, *5th Canadian international Petroleum conference*, Calgary, Alberta, Canada, June.

Pruess, K. and Tsang, Y. W. 1990. On two-phase relative permeability and capillary pressure of rough-walled rock fracture, *Water Resources Research*, 26(9): 1915-1926.

Reitsma, S. and Kueper, B. H. 1994. Laboratory measurement of capillary pressure-saturation relationship in a rock fracture, *Water Resources Research*, 30(4): 865-878.

Tsang, Y. W., And Tsang, C. F. 1989. Flow Channeling in a Single Fracture as a Two-Dimensional Strongly Heterogeneous Permeable Medium, *Water resources research*, 25(9): 2076-2080.

Walters, D. A. 1995. *The hydraulic and mechanical characterization of an oil sand fracture*, MSc thesis, University of Calgary, Calgary, Alberta.

Weerakone, W. M. S. B. and Wong, R. C. K. 2007. Determination of aperture distribution and DNAPL migration in a rough-walled rock fracture, *Proceedings of the 1st Canada-US rock mechanics symposium*, Vancouver, Canada, 27-31, May 2007, Taylor and Friends group, New York, USA.